Flat-Slab Thermal Structure and Evolution Beneath Central Mexico

Vlad C. Manea[1] and Marina Manea[1]

Abstract—Recent seismic and magnetotelluric experiments, aimed at better characterizing the shape and state of the subducting slab and continental crust beneath Central Mexico, exposed significant differences with conclusions of previous studies. A new slab geometry is revealed in which the subducting Cocos slab is perfectly flat between 120 to 290 km from the trench, after which it plunges into the asthenosphere at a dip angle of $\sim 65°$, in sharp contrast with the previously proposed $\sim 20°$ dip angle. Seismic tomography studies show negative P-wave velocity anomalies (-2 to -4%) in the mantle wedge beneath the Mexican Volcanic Belt, and positive anomalies ($+2$ to $+3\%$) for the subducted Cocos slab. Magnetotelluric experiments exposed a very low-resistivity area (1–10 Ωm) located within the continental crust just below the Mexican Volcanic Arc. Finally, several spots of non-volcanic tremors (NVTs) have been recorded inside the continental crust above the flat-slab segment. While all these experiments provide a better picture of the subduction system beneath Central Mexico, several key processes need further investigation. In this study, we take advantage of these new observations to better constrain the thermal structure beneath Central Mexico. Two different thermal models are computed for a mantle potential temperature (T_p) of 1,350 and 1,450°C, respectively. The new thermal structures are then converted into P-wave velocity anomalies and compared with the observed V_p anomalies. We found that a T_p of 1,450°C produced larger V_p anomalies that do not fit the observations. However, using a T_p of only 1,350°C, our predicted V_p anomalies are positive ($+2$ to $+3\%$) for the cold slab and negative (-2 to -4%) in the mantle wedge. These V_p estimates are consistent with the observed seismic tomography from P-wave arrivals, and therefore we conclude that a T_p of 1,350°C is a better estimate for the mantle potential temperature beneath Central Mexico. The new thermal model, in conjunction with phase diagrams for sediments, hydrated basalt and lithospheric mantle, have been used to estimate the amount and location of fluids released from the subducting Cocos slab. Several dehydration pulses have been identified along the slab interface where most of the fluids stored in sediments and oceanic crust are released into the overlying continental crust above the flat-slab. We found a good correlation between the pattern of these dehydration pulses and the location of NVTs, suggesting that slab dehydration is responsible for triggering the tremors. We suggest that NVT bursts localized above the flat slab segment represent the manifestation of ongoing continental crust hydration and weakening, a process that has been going on since 15 Ma ago when the Cocos slab entered into a flat-slab regime. Such continuous weakening would have reduced the suction forces that kept the slab in a flat regime in the last 15 Ma, allowing the slab to easily roll back. The continuous low-resistivity region recorded beneath the volcanic front in Central Mexico might represent the evidence of slab dehydration and crust weakening over time.

Key words: Flat-slab, thermal structure, Central Mexico, slab dehydration, slab rollback.

1. Introduction

Flat-slab subduction takes place at $\sim 10\%$ of the present-day convergent margins, in general where a correlation with buoyant plateaus and/or aseismic ridges exists (Cross and Pilger, 1982; McGeary et al., 1985; Gutscher et al., 2000). Nevertheless, such correlation does not exist in Central Mexico below the state of Guerrero, where a shallow subduction angle has been revealed at around 40–50 km depth and at distances up to ~ 250 km from the trench (Suarez et al., 1990). The slab geometry farther inland, beneath the Mexican Volcanic Arc, has been difficult to image because of the complete lack of intraslab seismicity. It was considered that from a distance of ~ 250 km from the trench the slab plunges into the asthenosphere at a shallow $\sim 20°$ angle, reaching a depth of around 100 km beneath the active Popocatepetl stratovolcano (Pardo and Suarez, 1995). This slab geometry was used by previous studies to infer and interpret the thermal structure in the area (Currie et al., 2002; Manea et al., 2004, 2005a). The period of flat-slab initiation in Mexico has been considered early-middle Miocene (Ferrari et al., 1999), but without upper plate deformation, as in the case of the Chilean flat-slab. Also, the initial flat-slab length is considered to have been larger in the past than it is today because the volcanic arc

[1] Computational Geodynamics Laboratory, Centro de Geociencias, Campus Juriquilla-Queretaro, Universidad Nacional Autonoma de Mexico, Mexico City, Mexico. E-mail: vlad@geociencias.unam.mx

migrated trenchward in the last 15 Ma at a rate of ∼10 km/Ma (FERRARI *et al.*, 2001).

In recent years, several studies and experiments have been carried out with the main purpose of exposing in great detail the subduction structure and state in this area. The Middle America Seismic Experiment (MASE) imaged the subducted Cocos plate beneath Central Mexico (CLAYTON *et al.*, 2007). The results from this research revealed a longer flat slab segment that extends further inland to ∼300 km from the trench, where then it sinks into the astheno-sphere at a steep angle of ∼65° (Fig. 1). Also, an ultra slow velocity layer, ∼3–5 km thick, interpreted as relict serpentinized mantle, was found on top of the flat-slab segment (PEREZ-CAMPOS *et al.*, 2008; SONG *et al.*, 2009). On the same profile, several regions of non-volcanic tremors (NVTs) have been identified above the flat-slab, with the majority of tremors con-centrated in an area located ∼220–240 km from the trench within the overriding continental crust (PAYERO *et al.*, 2008). NVTs are long-period low-frequency events with periods of several weeks, and are sus-pected to involve a chain reaction of small fractures caused by super-critical fluids (OBARA, 2002; KODAIRA *et al.*, 2004). Although the processes that generate NVTs are not well understood, in southwest Japan the

good agreement of the NVTs with the shape and position of the seismogenic zone confirm a tectonic origin for these vibrations (OBARA, 2002; JULIAN, 2002). The places where NVTs have been positively identified include Nankai, Cascadia and Mexico sub-duction zones, where young plates produce abundant fluids from the dehydration of sediments and metaba-salt (DRAGERT *et al.*, 2004). In the Nankai subduction zone, NVTs have been located near the seismic-aseismic transition zone (OBARA, 2002; SHELLY *et al.*, 2006; NUGRAHA and MORI, 2006; MIYAZAWA *et al.*, 2008). Also, apparently there is no kinetic delay in triggering NVTs; the speed at which these tremors move can reach 9 km/day, and might reflect the migration of fluids released by metamorphism (JULIAN, 2002). The fluid release from the subducting slab is the most common explanation for the origin of NVTs and this could be the case for Central Mexico, too. For this reason, a better-constrained thermal model is a useful tool to predict accurately where the slab dehydrates, and whether or not there is a correlation with the location of recorded NVTs.

The tomographic study of GORBATOV and FUKAO (2005) shows low-velocity regions (−2%) (probably mantle wedge) beneath the Mexican Volcanic Arc and high-velocity areas (+2%) corresponding to the subducted slab. Additionally, a low velocity area is revealed beneath the Cocos plate close to the trench, possibly attributed to the young (∼13–14 Ma) incoming Cocos plate. A similar recent study (YANG *et al.*, 2009), but farther west and with higher reso-lution, shows negative P-wave perturbations in the mantle wedge (−2 to 4%) and positive perturbations (+2 to +4%) interpreted as the subducted Cocos and Rivera plates. Since these seismic anomalies are often interpreted as thermal anomalies, they can be used to better constrain the thermal structure of a subduction zone (MANEA *et al.*, 2005b).

A magnetotelluric (MT) experiment, performed along the same profile as MASE, exposed a contin-uous high-conductive low-resistivity region located beneath the volcanic arc and in the continental crust (JÖDICKE *et al.*, 2006). These low-resistivity areas are interpreted as a consequence of fluid release from the subducting slab or partial melt, and therefore can provide insights about the past dynamics of the sub-duction system in Central Mexico.
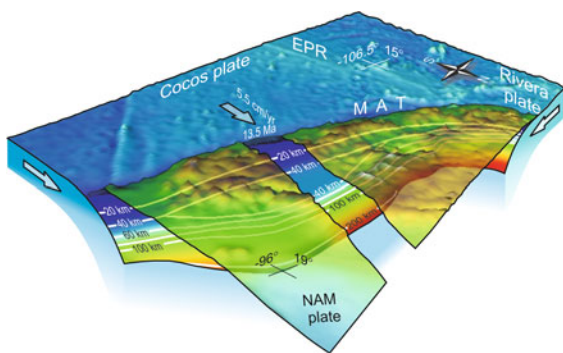

Figure 1

Three-dimensional visualization of the Mexican subduction zone from the northeast. Surface relief is shown as a semi-transparent layer. Labeled *white contours* and *color* gradation of the subducting plate indicate depths to the slab surface from the Earth's surface (PARDO and SUREZ, 1995; PEREZ-CAMPOS *et al.*, 2008). *Bold arrow* shows the direction of the Cocos Plate movement relative to North America. *EPR* East Pacific Rise, *MAT* Middle America Trench, *NAM plate* North America plate. Band cut through the surface relief is located above the flat-slab in Central Mexico where we performed the 2D numeric modeling

In this paper, we provide a new 2D steady-state thermal structure for Central Mexico, constrained by the new slab geometry and recent P-wave seismic tomography. Also, we explore the implications of slab dehydration in light of recently discovered NVTs. Based on the MT results and the NVT patterns we propose a time–space evolutionary model of the flat-slab since the Miocene in Central Mexico.

2. Thermal Models, Mantle Potential Temperatures and Seismic Tomography

2.1. Thermal Models

Using the numeric procedure proposed by MANEA et al. (2004) and the new slab geometry constrained from MASE, we estimated the 2D temperature distribution along the MASE profile for two possible mantle potential temperatures, 1,350 and 1,450°C. Other parameters are kept the same as in previous studies (MANEA et al., 2004, 2005a), including Cocos plate age and convergence rate of 13.7 Myr and 5.5 cm/yr, respectively, and a high pore pressure ratio along the subduction interface of 0.98. The pore pressure ratio effect is considered only along the plate interface from the trench to the hinge point, where the slab plunges abruptly into the mantle. The high pore pressure ratio between the oceanic and continental plates is consistent with the ultraslow velocity, high pore fluid pressure (HPFP) layer found on top of the subducted Cocos plate by SONG et al. (2009). The pore pressure ratio (PPR) controls the position of the 450°C isotherm, which represents the transition from partially coupled zone to stable sliding (HYNDMAN and WANG, 1993). According to GPS studies in Central Mexico the transition zone is located 200–220 km from the trench (KOSTOGLODOV et al., 2003). In our modeling, we used a PPR value of 0.98, which positions the 450°C isotherm at ~200 km from the trench (Fig. 2). The mantle wedge above the slab has a temperature-dependent viscosity, with a reference viscosity of 10^{21} Pa s and an activation energy for olivine of 300 kJ/mol (MANEA et al., 2004). The subducting slab drives the mantle wedge flow and there is no additional flow induced by slab rollback.

2.2. Mantle Potential Temperatures

Mantle potential temperature (T_p) is the temperature of mantle volume that rises towards the Earth's surface along an adiabat without melting (McKENZIE and BICKLE, 1988). Estimates of T_p range from 1,280 to 1,310°C (McKENZIE and BICKLE, 1988; PRESNALL et al., 2002) to 1340–1475°C (HERZBERG and O'HARA, 1998; PUTIRKA, 1999; GREEN et al., 2001; PUTIRKA, 2005). Using petrological and geochemical characteristics of primitive basalts, picrites, and komatiites, PUTIRKA et al. (2007) show that ambient mantle temperatures at normal oceanic ridges are in the range of 1,280–1,400°C, and that they can be even as high as 1,460°C below present-day Iceland.

We modeled the thermal structure beneath Central Mexico using two different T_p values, 1,350 and 1,450°C. The modeling results show that the mantle wedge above the slab is the most influenced by the T_p value (Fig. 2a, b). However, in both cases we predict melting of wet peridotite beneath the volcanic arc, and it is uncertain which T_p represents a better fit for the mantle potential temperature. In this case, we used an indirect method to better constrain T_p in our models. We converted the temperature distribution into synthetic V_p anomalies (MANEA et al., 2005b), and then we compared the results with the observed V_p anomalies in Mexico (GORBATOV and FUKAO, 2005; YANG et al., 2009).

2.3. Seismic Tomography in Central Mexico

Negative velocity anomalies in the mantle wedge above subducting slabs are interpreted as thermally induced structures (TAMURA et al., 2002). GERYA et al. (2006) developed a coupled petrological–thermomechanical model that permits prediction of seismic velocity anomalies in subduction zones. In this study, we employ a similar, but simplified approach from MANEA et al. (2005b) to predict seismic velocity anomalies (V_p) beneath Central Mexico using only the temperature dependence of seismic wave velocity from KARATO (1993). The predicted V_p perturbations are calculated relative to the PREM model (DZIEWONSKI and ANDERSON, 1981). We compared the predicted V_p anomalies with the results from several recent tomographic studies in Mexico in order to
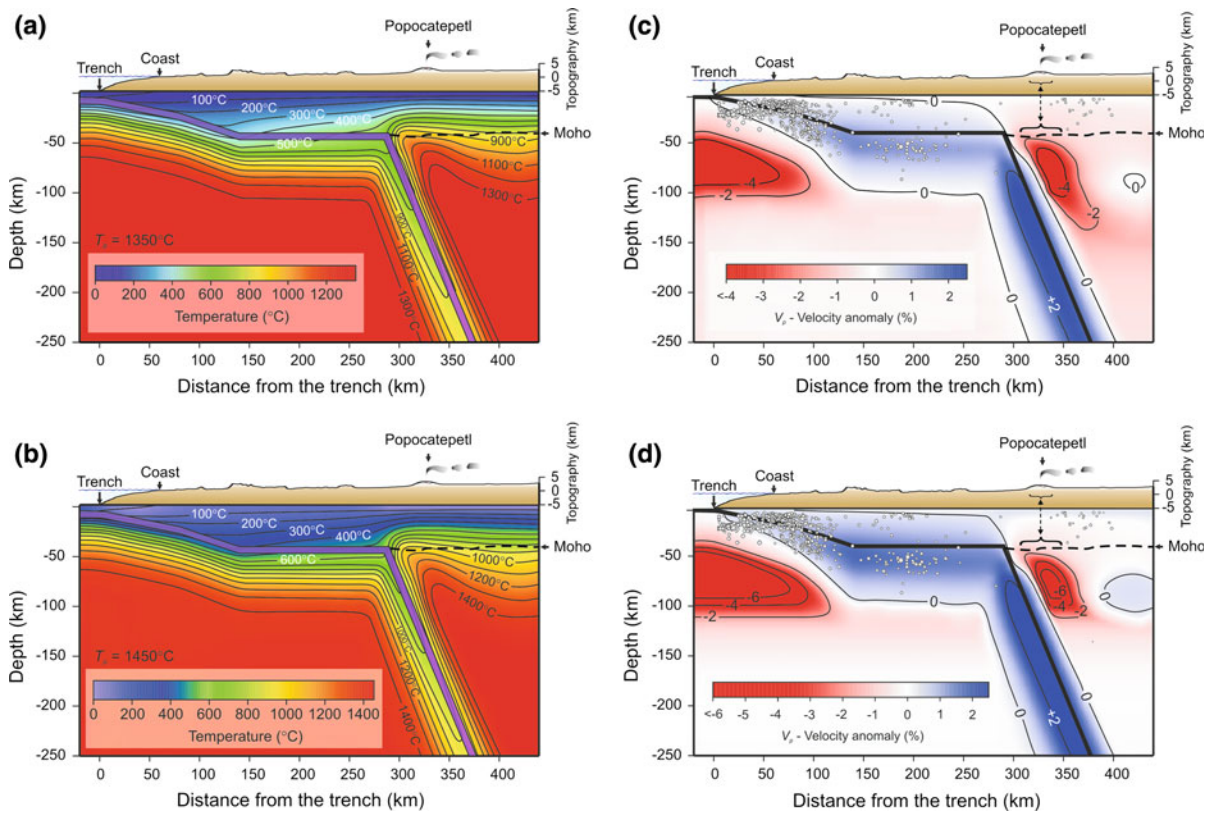
Figure 2
Predicted thermal models and V_p anomaly beneath Central Mexico. **a** Thermal model for $T_p = 1{,}350°C$. **b** Thermal model for $T_p = 1{,}450°C$. *Purple band* drawn over thermal model depicts the oceanic crust. **c** V_p velocity anomaly estimation from the temperature model with $T_p = 1{,}350°C$. **d** V_p velocity anomaly estimation from the temperature model with $T_p = 1{,}450°C$. *White circles* are the projection of earthquake hypocenters ($M > 4$) from SSN catalog for 2005–2006 epoch. *Solid* and *dashed black lines* illustrate the Cocos-North America plates interface and Moho from PEREZ-CAMPOS *et al.* (2008)

better constrain the thermal structure. As an input parameter, we used the thermal structure calculated for the two different T_p values, 1,450 and 1,350°C (Fig. 2a, b). The modeling results are presented in Fig. 2c, d and both show strong negative V_p anomalies in the mantle wedge and beneath the incoming Cocos plate in the range of −2 to −6%. Observed V_p anomalies in the wedge are in the range −2 to −4%, and therefore the best fitting model is obtained when we use a T_p of 1,350°C (Fig. 2c). Also, our modeling result (Fig. 2c) is consistent with the P-wave tomography of GORBATOV and FUKAO (2005), although the magnitude of the P-wave velocity anomaly estimated from thermal modeling (−4%) is higher than the observed one (−2%). However, a recent seismic experiment located few hundred km to the north from

Guerrero, (YANG *et al.*, 2009) shows P velocity perturbations in the mantle wedge up to −4%. In our modeling the cold slab induces a positive velocity anomaly of ∼+2%, a value consistent with both tomographic studies mentioned above, and also with the recent tomographic image from PEREZ-CAMPOS *et al.* (2008).

The negative velocity anomaly associated with mid-ocean ridges and young plates, as the Cocos and Rivera plates offshore from Mexico, is a common feature in global or regional seismic tomography (GUNG and ROMANOWICZ, 2004). Such a negative anomaly can also be observed beneath the incoming Cocos plate (GORBATOV and FUKAO, 2005 and also in our predicted V_p tomography inferred from temperature as seen in Fig. 2c, d).

3. Slab Dehydration

The water carrier in active subduction systems is the oceanic plate composed of sediments, oceanic crust and mantle layers. The young Cocos plate has a thin sediment layer only ~ 200 m thick, but most of these hydrated sediments enter into the subduction system (MANEA et al., 2003). Based on the newly constrained thermal model (Fig. 2a) and phase diagrams for sediment-, basalt-, and peridotite-water systems from RÜPKE et al. (2004), we analyze the stability of hydrous phases and estimate the water content in the subducting Cocos plate. We also explore the locations where various hydrous phases break down, and compare them with the position of NVTs and low-resistivity areas.

3.1. Sediment-water System

Figure 3a presents the estimation of H_2O amount retained by minerals in sediments as function of $P–T$ along the top slab interface. Sediments start to dehydrate at ~ 35 km depth and ~ 100 km from the trench where they drop from 4% wt. H_2O to 3.5% wt. H_2O. Then there are several similar dehydration pulses located along the flat-slab. A second pulse of 0.5% H_2O is released at 160–170 km from the trench and a third and larger one ($\sim 1\%$ H_2O) at 230–240 km from the trench. The location of these two former dehydration pulses corresponds with the position of areas of intense NVTs activity. The last dehydration pulse (0.5% H_2O) is located at 270–280 km from the trench just before the slab starts plunging into the asthenosphere. At a distance of ~ 300 km from the trench the sedimentary layer dehydrates $\sim 75\%$, and a total of $\sim 3\%$ wt. H_2O is released mostly above the flat-slab area (Fig. 4, inset). The remaining 1% wt. H_2O is carried down into subduction zone, where it can contribute to the water content of the upper mantle (ONO, 1998).

3.2. Basalt-water System

To estimate the water content stored in the basaltic oceanic crust, we use the phase diagram for metabasalt (RÜPKE et al., 2004) and top and bottom oceanic crust isotherms from the best-fit thermal

model (Fig. 2a). The results are presented in Fig. 3b, and show that no dehydration occurs before the slab enters into the flat regime. Even then, the slab runs for another ~ 100 km, when a large dehydration pulse goes off the slab at 230–240 km from the trench (Fig. 4). In this narrow band, the oceanic crust dehydrates $\sim 85\%$ and more than 3% wt. H_2O is released into the overriding continental crust. The location of this major dehydration pulse corresponds with the area where $\sim 80\%$ of the NVT bursts occur (Fig. 4). Also, this region overlaps with a smaller dehydration pulse ($\sim 1\%$ wt. H_2O) from sediments. The remaining 0.5% wt. H_2O stored in the basaltic crust is later released into the mantle wedge at a depth of ~ 90 km, below the active Popocatepetl volcano.

3.3. Peridotite-water System

The peridotite layer of oceanic plates represents one of the major water sources that are carried down in active subduction systems. We estimate the H_2O amount stored into the serpentinized subducting lithosphere beneath Central Mexico using two slab geotherms, located at the base of oceanic crust and 7 km below, and the phase diagram for serpentinized mantle (RÜPKE et al., 2004). The results presented in Fig. 3c show that a significant amount of water (6.5 wt%) is preserved in the serpentinized peridotite layer down to 60–70 km depth. The first dehydration occurs in the flat slab segment when for the same pressure the temperature increases above 500°C. Here only 0.5% is released and the dehydration front is distributed sub-horizontally for a distance of about 50 km beneath the first cluster of NVTs (Fig. 4). At greater depths, the slab crosses the choke point at 600–700°C at ~ 2 GPa (60–70 km depth) and a strong dehydration process occurs where $\sim 90\%$ of the fluid stored is released into the overlying mantle wedge through the oceanic crust. The slab depth beneath Popocatepetl is ~ 120 km, and the difference between this depth and the depth where the serpentinized oceanic lithosphere releases fluids ($\sim 60–70$ km), can be explained by the time necessary for the released water to cross the oceanic crust and sediments and to run off the slab into the overlying mantle at ~ 120 km depth. We conclude that this significant amount of H_2O released through
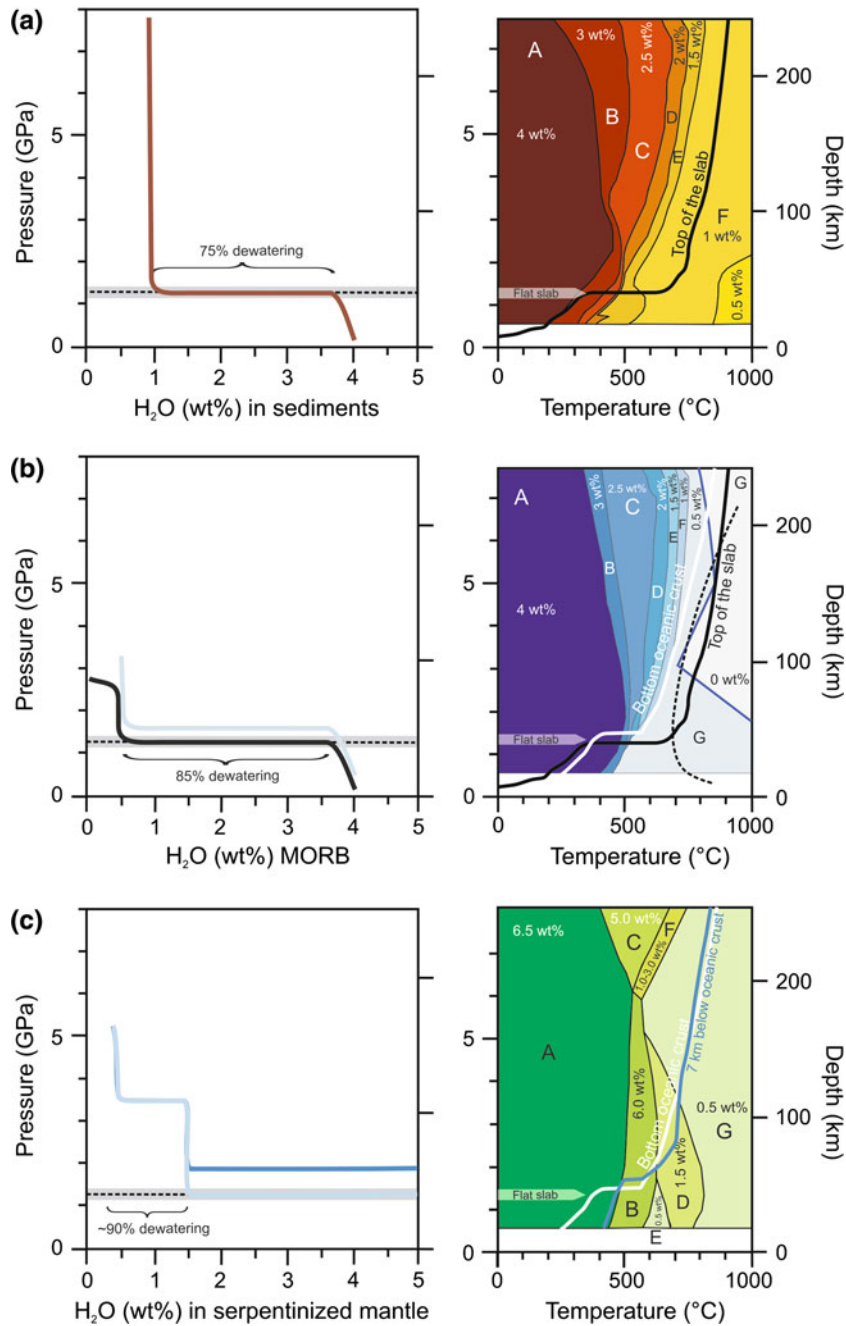
Figure 3
Computed phase equilibria and *P–T* water content for sediments (**a**), metabasalt (**b**), and serpentinized mantle (**c**). *Black*, *white* and *blue* *curves* represent the geotherms, all from the thermal model shown in Fig. 2a, at the *top* of the slab, the *bottom* of the oceanic crust, and 7 km below the oceanic crust, respectively. The plots on the *left* side illustrate how much H_2O (%) is released in each layer

slab deserpentinization can induce partial melting of the mantle above the slab and explain the volcanic productivity and the reasonably high H_2O found in the erupted mafic magmas, similar to magmas from other arcs (ROBERGE *et al*., 2009; CERVANTES and WALLACE, 2003).
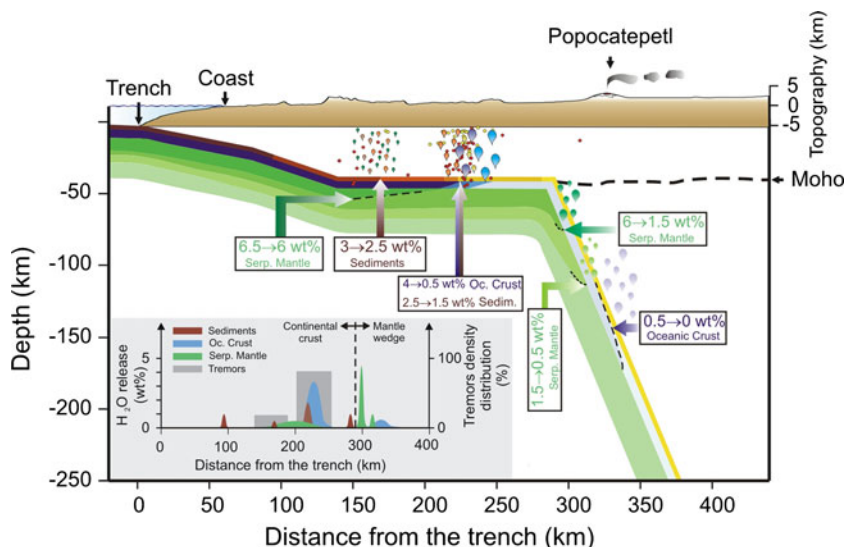
Figure 4

Sediments, oceanic crust, and serpentinized mantle dehydration along the subducting Cocos slab beneath Central Mexico. *Red* and *yellow dots* are the location of NVTs from PAYERO *et al.* (2008). *Colored drops* illustrate where the oceanic sediments, crust and serpentinized mantle dehydrate the most. *Inset plot* shows the location of the main dehydration pulses and NVTs along the slab interface. Note the good correlation between the position of dehydration episodes and the location of *NVT* bursts

4. Discussion and Conclusions

In this study, we combine our modeling results with results from recent experiments in Central Mexico to interpret key processes related to flat-slab subduction structure and dynamics. Here we computed a 2D steady-state thermal model; more realistic time-dependent 2D or 3D thermal models are proposed for future studies. However, despite the limitations of steady-state models, the new thermal structure presented here is well constrained by both GPS deformation studies (KOSTOGLODOV *et al.*, 2003) and seismic experiments (GORBATOV and FUKAO, 2005; PEREZ-CAMPOS *et al.*, 2008), and therefore it provides a reliable picture of the present-day thermal structure.

In the next sections, we provide a scenario of how slab dehydration could control and affect the resistivity distribution in the upper crust and could affect NVT patterns. Finally, we propose an evolution model for the flat-slab in Central Mexico for the last 15 m.y. based on present-day geophysical and past geological data.

4.1. Slab Dehydration, NVTs and Crust Resistivity

As shown in Sect. 3, the subducted oceanic crust and sediment layers are able to release significant fluids into the overlying continental crust. Additionally, the dehydration process occurs in several pulses that differ both in location and the amount of H_2O released (Fig. 4, inset). The major discharge is located in a narrow band, 230–250 km from the trench, where both sediments and oceanic crust strongly dehydrate, and a total amount of $\sim 4\%$ wt. H_2O is flushed into the continental crust. This narrow band corresponds with the area where most of the NVT activity occurs. Actually, $\sim 80\%$ of the NVT bursts are recorded in this spot, strongly suggesting that slab dehydration is the main controlling source of tremors distribution above the flat-slab in Central Mexico. The other region where a smaller number of NVTs were recorded is situated closer to the trench at $\sim 150–180$ km. In this area we found that only a small amount of fluids (0.5% wt. H_2O) is released from oceanic minerals breakdown reactions.

The triggering mechanism of NVTs depends on where and how fluids are distributed along the subducting slab interface, and several mechanisms have been proposed. For example, for southwest Japan, MIYAZAWA *et al.* (2008) suggested that normal stress reduction accompanied by horizontal compression can trigger these tremors. However, for the Cascadia subduction zone, shear stress changes

from Love waves are proposed to induce NVTs (RUBINSTEIN *et al.*, 2010). These observations could indicate a difference in physical properties between the two subduction regions. MIYAZAWA *et al.* (2008) proposed that the fluid pattern on and off the fault plane actually controls the triggering mechanism. A homogenous fluid distribution along the slab interface would favor normal stress reduction, whereas a more heterogeneous fluid distribution could induce a shear strain change. In Central Mexico, we observed two distinct locations where NVTs occur and where the subducting Cocos plate undergoes dehydration (Fig. 4). This fluid pattern favors the first triggering mechanism where normal stress reduction coupled with horizontal compression could effectively induce NVTs.

In our interpretation, we take advantage of the magnetotelluric survey in Central Mexico carried out by JÖDICKE *et al.* (2006). High-conductive low-resistivity (<10 Ωm) areas imaged by MT surveys are often interpreted as zone rich in fluids (OGAWA *et al.*, 2001; RYBIN *et al.*, 2004; SOYER and UNSWORTH, 2006). In general, the overall resistivity of a rock is considered as the sum of both solid grains and pore

spaces saturated with fluids. Moreover, if the fluids contain dissolved ions, the resistivity of the fluid part decreases further because the ions can easily move. Also, low-resistivity of rocks could be due to interconnected grain boundary phases such as water, partial melts, sulphides or graphite (SCHILLING *et al.*, 1997; JONES, 1999). Magnetotelluric exploration of the San Andreas Fault has revealed that the fault is characterized by a low-resistivity wedge (~ 3 Ωm) (UNSWORTH *et al.*, 1997), which has been attributed to aqueous pore fluids that dominate the resistivity of most rocks around the fault. The continental crust above the subducted slab in Central Mexico is mostly characterized by high resistivity. However, an isolated low-resistivity (~ 50 Ωm) spot can be identified at ~ 100 km from the trench at a depth of 20–30 km. From our modeling results, this area corresponds to the first dehydration pulse from the sedimentary layer (Fig. 5), and we interpret this low-resistivity area as a result of sediment dehydration. The continental crust beneath the volcanic arc is characterized by low-resistivity (1–10 Ωm) distributed in a ~ 300-km long band. This LR band ends where the NVT area is located above the eastern end of the flat-slab segment
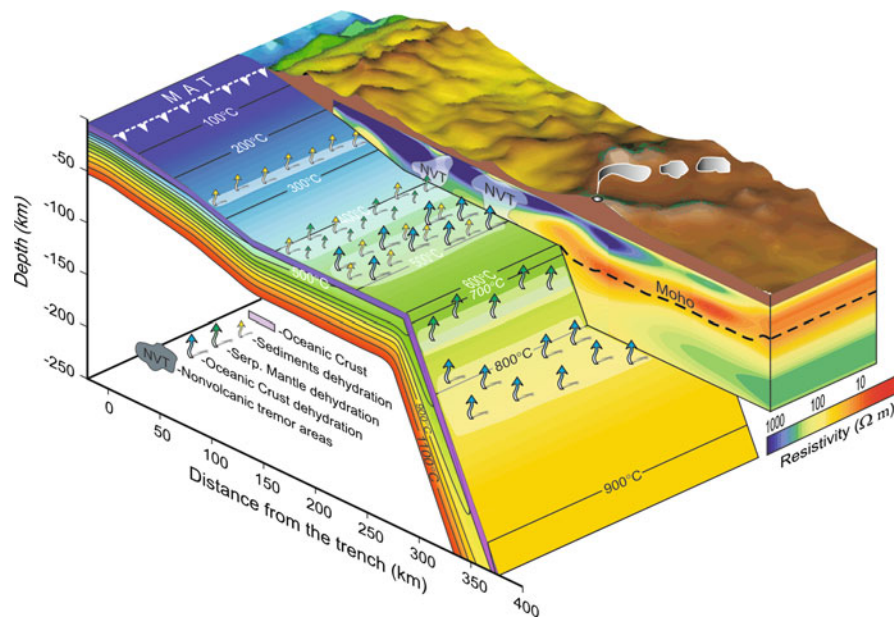

Figure 5
3D view of the flat-slab subduction in Central Mexico. The slab surface is shown in *color shades* that correspond to the temperature model from Fig. 2a. *Yellow*, *blue* and *green arrows* on the slab surface represent the locations where oceanic sediments, crust and serpentinized mantle dehydrate. The background image cut through the continental crust is the resistivity model of JÖDICKE *et al.* (2006)

(Fig. 5). We interpret this elongated low-resistivity region as a consequence of continuous subducting slab dehydration over the last 15–20 Ma. In fact, FERRARI (2004) shows that the Mexican Volcanic Belt has migrated trenchward at a rate of ∼10 km/Myr, probably implying that the slab has rolled back and the length of the flat-slab segment has diminished since the Miocene. Similar low-resistivity in the overriding crust has been imaged above the flat slab region in central Chile, where an MT survey revealed a continuous conductive region in the continental crust at ∼25 km depth and above the flat slab (BOOKER et al., 2004). On the other hand, the MT survey performed for the Cascadia subduction zone, which did not experienced flat-slab and rollback, shows high resistivity areas in the continental crust (100–1,000 Ωm) with only some small-scale low-resistivity spots above the Moho. These low-resistivity localized areas are interpreted as the consequence of aqueous fluids released from the subducting Juan de Fuca slab (SOYER and UNSWORTH, 2006).

The difference in the low resistivity pattern between the two types of subducting slabs suggests that the flat slab dewatering followed by rollback causes the MT anomaly recorded in central México beneath the volcanic arc (Fig. 5). However, the nature of this low resistivity area could also be interpreted in terms of partial melt. The temperatures (800–1,000°C) predicted for the lowermost continental crust beneath the volcanic arc (Fig. 2a, b) are well above the wet melting temperatures for a wide range of lower crustal rock types, therefore there could be partial crustal melting in that area. In the western US during the Laramide orogeny, a slab rollback process, similar to what we proposed here, likely led to voluminous crustal melting and created widespread rhyolitic eruptions. In the area of the Tepic-Zacoalco graben, the first episodes of voluminous rhyolithic volcanism started in the late Miocene (∼7 Ma) and continued in the early Pliocene and late Pliocene-Quaternary (GÓMEZ-TUENA et al., 2007). Also, it is worth mentioning that this rhyolithic manifestation coincides with the trenchward migration of the volcanic front. However, the solidification of partial melt at the base of the crust could also induce the accumulation of large amounts of fluids that could explain the observed low-resistivity anomaly beneath the arc and backarc (SOYER and UNSWORTH, 2006). Although partial melt in the lower crust might somehow explain the low-resistivity area beneath the volcanic arc, part of this electric anomaly is located above the eastern end of the flat-slab segment where our thermal models predict temperatures as low as 400°C. A combination of interconnected partial melts and fluids in the lower crust would explain the exceptionally low-resistivity (∼1 Ωm) recorded beneath the volcanic arc and above the flat-slab in Central Mexico (Fig. 5).

4.2. Crust Weakening, Suction Forces and Slab Rollback

In active subduction systems, the slab geometry reflects the balance of slab pull, elastic resistance and hydrodynamic forces (suction forces) in the mantle wedge (PEREZ-GUSSINYÉ et al., 2008; MANEA and GURNIS, 2007). Whereas the slab density excess, with respect to the surrounding mantle, controls slab pull force, the suction forces act as a counterbalance force which is mainly controlled by the mantle wedge viscosity. MANEA and GURNIS (2007) show how mantle wedge viscosity affects the slab dip evolution in an active subduction zone. A low viscosity wedge tends to increase the slab dip, whereas a high wedge viscosity decreases the subduction angle and can even produce flat-slabs. In the latter case, the suction forces in the mantle wedge are sufficiently high to compensate the slab positive buoyancy. Thus, elevated suction forces along the slab-mantle interface could sustain long-lived flat-slab systems. This is likely the case in Central Mexico, where flat-slab subduction has been going on since the Miocene (FERRARI et al., 1999). Geological evidence shows that since the Miocene the volcanic arc has moved slowly trenchward at a rate of ∼10 km/Myr (FERRARI, 2004), suggesting slab rollback and flat-slab shortening mechanisms. Rollback of the subducted Cocos plate over the last 2 Myr has been proposed to explain high-Nb alkali basaltic magmas for the Michoacan-Guanajuato Volcanic Field located only several hundreds of km to the west of our study area (JOHNSON et al., 2009). Integrating these observations with the 2D thermo-mechanical model of the subduction zone beneath Central Mexico, we propose the following scenario for flat-slab evolution:

1. When flat-slab started in Mexico around 15 Ma ago, the flat segment length was larger than today, extending probably some 450 km from the trench (Fig. 6a). This assumption is supported by the age data for mafic rocks in Central Mexico (FERRARI, 2004). The main reason for initiating such a long flat-slab is still unknown.

2. A continuous process of slab dehydration at the eastern end of the flat-slab segment weakens the base of the continental crust (Fig. 6b). Numerical simulations support the assumption that slab dehydration facilitates significant weakening of the overriding plate (ARCAY et al., 2006). In Central Mexico, a low-resistivity area can now
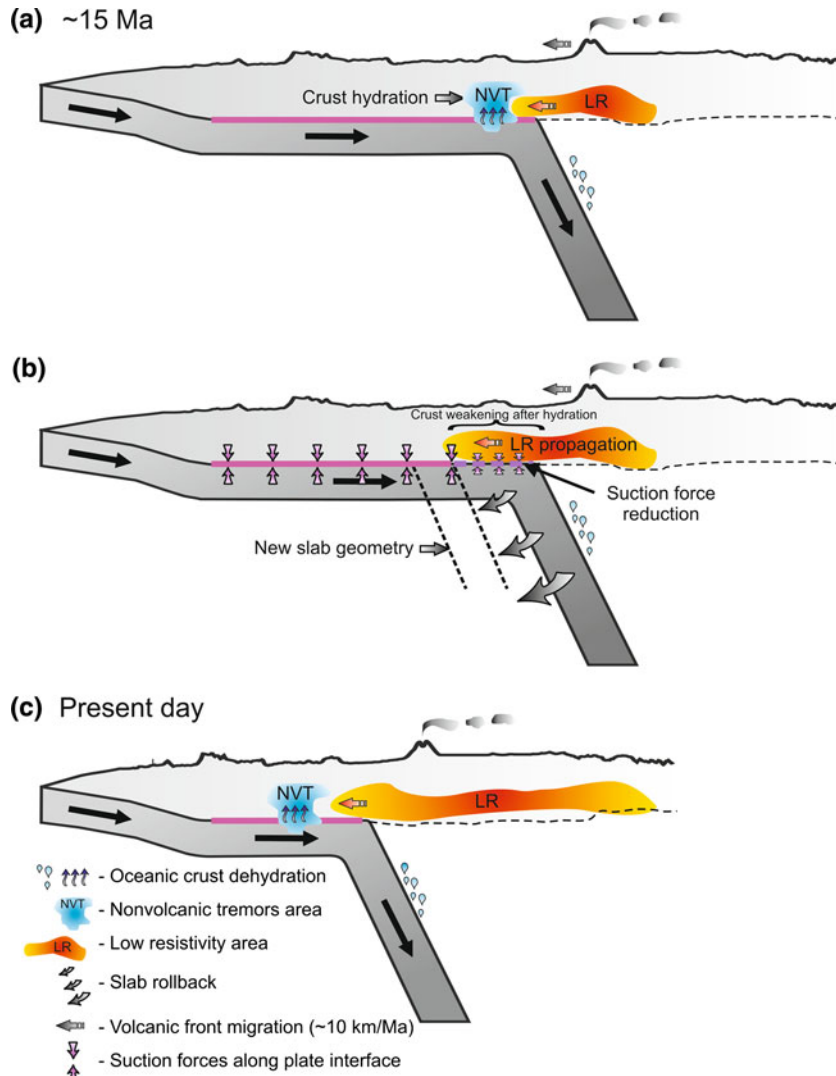

Figure 6
Theoretical evolutionary model proposed for the flat-slab subduction beneath Central Mexico. **a** A longer flat-slab segment could have existed ~15 Ma ago. Over time, slab dehydration weakens the overriding continental crust. *NVT*s can be an indication of the weakening process. **b** Once the crust is sufficiently weakened, the magnitude of the suction force that kept the subducting Cocos plate in flat-slab regime diminishes, allowing the slab to roll back. As a consequence, the volcanic arc and the low-resistivity area (*LR*) start propagating trenchward. **c** In time, the length of the flat-slab section reduces, the *LR* area propagates even further until the slab takes the present day geometry as revealed by MASE. *NVT* bursts still occur at present, suggesting that crust weakening is an ongoing process

propagate trenchward into the newly weakened and hydrated crust. We propose that such a prolonged flat-slab dehydration regime might have weakened the overriding continental crust enough to allow the slab to start rollback. The actual process behind the slab rollback and overlying crust weakening is still unknown. However, slab rollback permits the hot mantle wedge to flow back into the newly created space, explaining why the volcanism migrated trenchward. In our view, continuous weakening of the continental crust above the flat-slab segment leads to a significant reduction in viscosity, and therefore suction forces, allowing the slab to decouple from the continental plate (MANEA and Gurnis, 2007; PEREZ-GUSSINYÉ et al., 2008).

3. We propose that slab rollback occurs in steps, and several episodes of crust weakening and slab rollback lead to the present day subduction geometry in Central Mexico (Fig. 6c). Present day strong NVTs above the flat-slab would be the manifestation of ongoing hydration and weakening processes, that will eventually promote another episode of slab rollback in the future.

Acknowledgments

REFERENCES

ARCAY, D., DOIN, M.-P., TRIC, E., BOUSQUET, R., and DE CAPITANI, C. (2006), Overriding plate thinning in subduction zones: localized convection induced by slab dehydration, *Geochem. Geophys. Geosyst.* 7, Q02007. doi:10.1029/2005GC001061.

BOOKER, J., FAVETTO, A., and POMPOSIELLO C. (2004), Low electrical resistivity associated with plunging of the Nazca flat slab beneath Argentina. *Nature* 429, 399–403.

CERVANTES, P. and WALLACE, P. (2003), Role of H_2O in subduction zone magmatism: new insights from melt inclusions in high-Mg basalts form central Mexico. *Geology* 31, 235–238.

CLAYTON, R. W., DAVIS, P. M., and PEREZ-CAMPOS, X. (2007), Seismic structure of the subducted Cocos plate. *Eos Trans. AGU, Jt. Assem. Suppl.* 88(23), Abstract T32A-01.

CROSS, T. A. and PILGER R. H. Jr. (1982), Controls of subduction geometry, location of magmatic arcs, and tectonics of arc and back-arc regions. *Geol. Soc. Am. Bull.* 93, 545–562.

CURRIE, C. A., HYNDMAN, R. D., WANG, K. and KOSTOGLODOV, V. (2002), Thermal models of the Mexico subduction zone: Implications for the megathrust seismogenic zone, *J. Geophys. Res.* 107(B12), 2370. doi:10.1029/2001JB000886.

DRAGERT, H., WANG, K., and ROGERS, G. (2004), Geodetic and seismic signatures of episodic tremor and slip in the northern Cascadia subduction zone. *Earth Planets Space* 56, 1143–1150.

DZIEWONSKI, A. M. and ANDERSON, D. L. (1981), Preliminary reference Earth model. *Phys. Earth. Planet. Int.* 25, p 297–356.

FERRARI, L. (2004), Slab detachment control on mafic volcanic pulse and mantle heterogeneity in central Mexico, *Geology* 32, 77–80.

FERRARI L., LOPEZ-MARTINEZ M., AGUIRRE-DIAZ G., and CARRASCO-NUÑEZ, G. (1999), Space-time patterns of Cenozoic arc volcanism in central Mexico: from the Sierra Madre Occidental to the Mexican Volcanic Belt. *Geology* 27, 303–306.

FERRARI, L., PETRONE, C. M., and FRANCALANCI, L. (2001), Generation of oceanic-island basalt-type volcanism in the western Trans-Mexican volcanic belt by slab rollback, asthenosphere infiltration, and variable flux melting, *Geology* 29, 507–510.

GERYA, V. T., CONNOLLY, J. A. D., YUEN, A. D., GORCZYK, W., and CAPEL, A. M. (2006), Seismic implications of mantle wedge plumes. *Phys. Earth Planet. Interiors* 156, 59–74.

GÓMEZ-TUENA, A., OROZCO-ESQUIVEL, MA. T., and FERRARI, L. (2007), Igneous petrogenesis of the trans-mexican volcanic belt, In: Alaniz-Álvarez, S. A., and Nieto-Samaniego, Á. F. (eds.) Geology of México: celebrating the centenary of the Geological Society of México: *Geological Society of America Special Paper* 422, 129–181. doi:10.1130/2007.2422(05).

GORBATOV, A. and FUKAO, Y. (2005), Tomographic search for missing link between the remnant Farallon slab and present Cocos subduction. *Geophys. J. Int.* 160, 849–854.

GREEN, D. H., FALLOON, T. J., EGGINS, S. M., and YAXLEY, G. M. (2001), Primary magmas and mantle temperatures, *Eur. J. Mineral.* 13, 437–451.

GUNG, Y. and ROMANOWICZ, B. (2004), Q tomography of the upper mantle using three component long period waveforms, *Geophys. J. Int.* 157, 813–830.

GUTSCHER, M. A., SPAKMAN, W., BIJWAARD, H., ENGDAHL, E. R. (2000), Geodynamics of flat subduction: seismicity and tomographic constraints from the Andean margin. *Tectonics* 19, 814–833.

HERZBERG, C., and O'HARA, M. J. (1998), Phase equilibrium constraints on the origin of basalts, picrites, and komatiites. *Earth Sci. Rev.* 44, 39–79.

HYNDMAN, R. D. and WANG, K. (1993), Thermal constraints on the zone of major thrust earthquake failure: the Cascadia subduction zone. *J. Geophys. Res.* B98, 2039–2060.

JÖDICKE, H., JORDING, A., FERRARI, L., ARZATE, J., MEZGER, K., and RUPKE, L. (2006), Fluid release from the subducted Cocos plate and partial melting of the crust deduced from magnetotelluric studies in southern Mexico: Implications for the generation of volcanism and subduction dynamics. *J. Geophys. Res.* 111, B08102. doi:10.1029/2005JB003739.

JOHNSON, E. R., WALLACE, P. J., DELGADO GRANADOS, H., MANEA, V. C., KENT, A. J. R., BINDEMAN, I. N., and DONEGAN C. S. (2009), Subduction-related volatile recycling and magma generation

beneath Central Mexico: insights from melt inclusions, oxygen isotopes and geodynamic models. *J. Petrol.* 50(9), 1729–1764.

JONES, A. G. (1999), Imaging the continental upper mantle using electromagnetic methods. *Lithos* 48, 57–80.

JULIAN, B. (2002), Seismological detection of slab metamorphism, *Science* 296, 1625–1626.

KARATO, S. I. (1993), Importance of anelasticity in the interpretation of seismic tomography. *Geophys. Res. Lett.* 20, 1623–1626.

KODAIRA, S., IIDAKA, T., KATO, A., PARK, J.-O., IWASAKI, T., KANEDA, Y. (2004), High pore fluid pressure may cause silent slip in the Nankai Trough. *Science* 304, 1295–1298.

KOSTOGLODOV, V., SINGH, S. K., SANTIAGO, J. A., FRANCO, S. I., LARSON, K. M., LOWRY, A. R., and BILHAM, R. (2003), A large silent earthquake in the Guerrero seismic gap, Mexico., *Geophys. Res. Lett.* 30(15), 1807. doi:10.1029/2003GL017219.

MANEA, V. C. and GURNIS, M. (2007), Subduction zone evolution and low viscosity wedges and channels, *Earth Planet. Sci. Lett.* 264, 1–2, pp 22–45.

MANEA, M., MANEA, V. C., KOSTOGLODOV, V. (2003), Sediment fill of the Middle America Trench Inferred from the gravity anomalies. *Geofis. Int.* 42 (4), 603–612.

MANEA, V. C., MANEA, M., KOSTOGLODOV, V., CURRIE, C.A. and SEWELL, G. (2004), Thermal structure, coupling and metamorphism in the Mexican subduction zone beneath Guerrero, *Geophys. J. Int.* 158, 775–784. doi:10.1111/j.1365-246X.2004.02325.x.

MANEA, V. C., MANEA, M., KOSTOGLODOV, V., and SEWELL, G. (2005a), Thermo-mechanical model of the mantle wedge in Central Mexican subduction zone and a blob tracing approach for the magma transport. *Phys Earth Planet Interiors* 149, 165–186. doi:10.1016/j.pepi.2004.08.024.

MANEA, V. C., MANEA, M., KOSTOGLODOV, V., and SEWELL, G. (2005b), Thermal models, magma transport, and velocity estimation beneath southern Kamchatka. In: Foulger, G. R., Natland, J. H., Presnell, D. C., and Anderson, D. L. (eds.), *GSA Special paper: plates, plumes and paradigms* 388–31, pp 517–536.

MCGEARY, S., NUR, A., BEN-AVRAHAM, Z. (1985), Spacial gaps in arc volcanism: the effect of collision or subduction of oceanic plateaus. *Tectonophysics* 119, 195–221.

MCKENZIE, D., and BICKLE, M. J. (1988), The volume and composition of melt generated by extension of the lithosphere, *J. Petrol.* 29, 625–679.

MIYAZAWA, M., BRODSKY, E. E., and MORI, J. (2008), Learning from dynamic triggering of low-frequency tremor in subduction zones. *Earth Planets Space* 60, e17–e20.

NUGRAHA, A. D. and MORI, J. (2006), 3-D velocity structure in the Bungo channel and Shikoku Area, Japan, and its relationship to low-frequency earthquakes, *Geophys. Res. Lett.* 33, L24307.

OBARA, K. (2002), Nonvolcanic Deep Tremor Associated with Subduction in Southwest Japan. *Science* 296, no. 5573, pp 1679–1681. doi:10.1126/science.1070378.

OGAWA, Y., MISHINA, M., GOTO, T., SATOH, H., OSHIMAN, N., KASAYA, T., TAKAHASHI, Y., NISITANI, T., SAKANAKA, S., UYESHIMA, M., TAKAHASHI, Y., HONKURA, Y., and MATSUSHIMA, M. (2001), Magnetotelluric imaging of fluids in intraplate earthquakes zones, NE Japan back arc, *Geophys. Res. Lett.* 28, 3741–3744.

ONO, S. (1998), Stability limits of hydrous minerals in sediment and mid-ocean ridge basalt compositions: implications for water transport in subduction zones. *J. Geophys. Res.* 103 (B8), 18253–18267.

PARDO, M. and SUAREZ, G. (1995), Shape of the subducted Rivera and Cocos plates in southern Mexico: seismic and tectonic implications, *J. Geophys. Res.* 100, 12357–12373.

PAYERO, J., KOSTOGLODOV, V., SHAPIRO, N., MIKUMO, T., IGLESIAS, A., PEREZ-CAMPOS, X., and CLAYTON, R. (2008), Non-volcanic tremor observed in the Mexican subduction zone. *Geophys. Res. Lett.* 35, L07305.

PEREZ-CAMPOS, X., KIM, Y. H., HUSKER, A., DAVIS, P. M., CLAYTON, R. W., IGLESIAS, A., PACHECO, J. F., SINGH, S. K., MANEA, V. C., and GURNIS, M. (2008), Horizontal subduction and truncation of the Cocos plate beneath central Mexico, *Geophys. Res. Lett.* 35, L18303. doi:10.1029/2008GL035127.

PEREZ-GUSSINYÉ, M., LOWRY, A., PHIPPS MORGAN, J., and TASSARA, A. (2008), Effective elastic thickness variations along the Andean margin and their relationship to subduction geometry. *Geochem. Geophys. Geosyst.* 9, 2.

PRESNALL, D. C., GUDFINNSON, G. H., and WALTER, M. J. (2002), Generation of mid-ocean ridge basalts at pressures from 1 to 7 GPa, *Geochim. Cosmochim. Acta* 66, 2073–2090.

PUTIRKA, K. (1999), CPX + Liquid equilibria. *Contrib Mineral Petrol.* 135, 151–163.

PUTIRKA, K. D. (2005), Mantle potential temperatures at Hawaii, Iceland, and the mid-ocean ridge system, as inferred from olivine phenocrysts: evidence for thermally driven mantle plumes, *Geochem. Geophys. Geosyst.* 6, Q05L08. doi:10.1029/2005GC000915.

PUTIRKA, K. D., PERFIT, M., RYERSON, F. J., and JACKSON, M. G. (2007), Ambient and excess mantle temperatures, olivine thermometry, and active vs. passive upwelling. *Chem. Geol.* 24, 177–206.

ROBERGE, J., DELGADO-GRANADOS, H., and WALLACE, P. J. (2009), Mafic magma recharge supplies high CO_2 and SO_2 gas fluxes from Popocatépetl volcano, Mexico. *Geology*, vol 37, no. 2, p 107–110. doi:10.1130/G25242A.1.

RUBINSTEIN, J. L., SHELLY, D. R., and ELLSWORTH, W. L. (2010), Non-volcanic tremor: a window into the roots of fault zones. In: Cloetingh, S., Negendank, J. (eds.), *New frontiers in integrated solid earth sciences.* International year of planet earth. , Springer Science + Business Media B.V. doi:10.1007/978-90-481-2737-5_8.

RÜPKE, L. H., MORGAN, J. P., HORT, M., CONNOLLY, J. A. D. (2004), Serpentine and the subduction zone water cycle. *Earth Planet. Sci. Lett.* 223, 17–34.

RYBIN, A., SPICHAK, V., BATALEV, V., SCHELOCHKOV, G., BATALEVA, E., and SAFRONOV, I. (2004), Magnetotelluric investigations of an active thrust faults in the Northern Tien Shan, Kyrgyzstan, Central Asia. IAGA WG 1.2 on electromagnetic induction in the earth. Available at *Proceedings of the 17th Workshop Hyderabad*, India, October 18–23.

SCHILLING, F. R., PARTZSCH, G. M., BRASSE, H., and SCHWARZ, G. (1997), Partial melting below the magmatic arc in the Central Andes deduced from geoelectromagnetic field experiments and laboratory data. *Phys. Earth Planet. Inter.* 103, pp 17–31.

SHELLY, D. R., BEROZA, G. C., IDE, S., and NAKAMULA, S. (2006), Low-frequency earthquakes in Shikoku, Japan, and their relationship to episodic tremor and slip, *Nature* 442, 188–191.

SONG, T. R. A., HELMBERGER, D. V., BRUDZINSKI, M. R., CLAYTON, R. W., DAVIS, P., PEREZ-CAMPOS, X., and SINGH, S. K. (2009), Subducting slab ultra-slow velocity layer coincident with silent earthquakes in southern Mexico, *Science* 324, 502–506.

SOYER, W. and UNSWORTH, M. (2006), Deep electrical structure of the northern Cascadia (British Columbia, Canada) subduction

zone: Implications for the distribution of fluids. *Geology*, vol 34, no. 1, p 53–56. doi:10.1130/G21951.1.

SUAREZ, G., MONFRET, T., WITTLINGER, G., and DAVID, C. (1990), Geometry of subduction and depth of the seismogenic zone in the Guerrero gap, Mexico. *Nature* 345, 336–338.

TAMURA, Y., TATSUMI, Y., ZHAO, D. P., KIDO, Y., and SHUKUNO, H. (2002), Hot fingers in the mantle wedge: new insights into magma genesis in subduction zones. *Earth Planet. Sci. Lett.* 197, pp 105–116.

UNSWORTH, M. J., MALIN, P. E., EGBERT, G. D., and BOOKER, J. R. (1997), Internal structure of the San Andreas Fault Zone at Parkfield, California. *Geology* 25, 359–362.

YANG, T., GRAND, S. P., WILSON, D., GUZMAN-SPEZIALE, M., GOMEZ-GONZALEZ, J. M., DOMINGUEZ-REYES, T., and NI, J. (2009), Seismic structure beneath the Rivera subduction zone from finite-frequency seismic tomography. *J. Geophys. Res*. 114, B1. doi: 10.1029/2008JB005830.